HHS Public Access

Author manuscript

Cancer Discov. Author manuscript; available in PMC 2022 January 01.

Published in final edited form as:

Cancer Discov. 2021 July ; 11(7): 1661–1671. doi:10.1158/2159-8290.CD-20-0896.

A chimeric GM-CSF/IL18 receptor to sustain CAR T-cell function

Shannon Lange[1,*], **Laurens GL Sand**[1,*], **Matthew Bell**[1], **Sagar L Patil**[1], **Deanna Langfitt**[1], **Stephen Gottschalk**[1]

[1]Department of Bone Marrow Transplantation and Cellular Therapy, St. Jude Children's Research Hospital, Memphis, TN 38105

Abstract

The inability of CAR T-cells to sustain their effector function after repeat exposure to tumor cells is a major obstacle to their success in patients with solid tumors. To overcome this limitation, we designed a novel chimeric cytokine receptor to create an autocrine loop that links activation-dependent GM-CSF production by CAR T-cells to IL18 receptor signaling (GM18). Expression of GM18 in CAR T-cells enhanced their effector function in an antigen- and activation-dependent manner. In repeat stimulation assays, which mimic chronic antigen exposure, CAR.GM18 T-cells had a significant greater ability to expand and produce cytokines in comparison to their unmodified counterparts targeting EphA2 or HER2. *In vivo*, CAR.GM18 T-cells induced tumor regression at cell doses at which standard CAR T-cells were ineffective in two solid tumor xenograft models. Thus, our study highlights the potential of hijacking cytokines that are physiologically secreted by T-cells to bolster their antitumor activity.

Keywords

T-cell immunotherapy; cancer; solid tumors; CAR; IL-18; GM-CSF

INTRODUCTION

The adoptive transfer of chimeric antigen receptor (CAR) T-cells has resulted in impressive clinical responses for a broad range of hematological malignancies including lymphoma, leukemia, and multiple myeloma (1). However, CAR T-cells had limited antitumor activity in patients with solid tumors (2) and faces many challenges, including identification of safe target antigens, improving homing to tumor sites, and enabling CAR T-cells to expand and persist in the setting of chronic antigen exposure (2).

CAR T-cell activation and proliferation requires a distinct set of signals, which consist of CAR-mediated antigen-specific CD3ζ activation and costimulation (e.g. CD28 or 4-1BB), resulting in cytokine production (1,2). However, the ability of CAR T-cells to produce

Corresponding author: Stephen Gottschalk, Department of Bone Marrow Transplantation and Cellular Therapy, St. Jude Children's Research Hospital, 262 Danny Thomas Place, MS321, Memphis, TN 38105, Phone: (901) 595-2166, stephen.gottschalk@stjude.org.
*Authors contributed equally to the studies in this manuscript

Conflict of interests: SL, LS, and SG have patent applications in the fields of T-cell and/or gene therapy for cancer. SG has a research collaboration with TESSA Therapeutics, is a DSMB member of Immatics, and on the scientific advisory board of Tidal.

cytokines is not sustained in repeat stimulation assays that mimic chronic antigen exposure, resulting in cell death after 2-3 rounds of antigen-specific stimulation (3). Several strategies are being explored to overcome this limitation. For example, CAR T-cells have been genetically modified to express cytokines or delete negative regulators (2). In addition, we and others have shown that an inducible costimulatory molecule that activates MyD88, the central signaling hub for toll-like receptors (TLRs) and the IL-1 and IL-18 receptors (4), sustains CAR T-cell effector function in the setting of chronic antigen exposure (3).

T-cells normally receive activation, costimulatory, and cytokine signals in a temporospatial manner. While investigators have developed synthetic signaling circuits to mimic this by linking expression of a gene to T-cell activation (5), we wanted to develop an antigen-dependent autocrine loop with molecules that are expressed in human cells. We took advantage of GM-CSF, a cytokine that is invariably expressed post CAR T-cell activation (3), and designed a chimeric cytokine receptor (GM18) that activates MyD88. It consists of the extracellular domains of the α/β chains of the GM-CSF receptor and the transmembrane and signaling domains of the α/β chains of the IL18 receptor. We demonstrate that expression of GM18 in CAR T-cells strikingly enhances their effector functions in the setting of chronic antigen exposure *ex vivo*. This translated into potent antitumor activity of CAR T-cells targeting EphA2 or HER2 in xenograft models.

RESULTS

Generation of CAR T-cells expressing a GM-CSF/IL-18 chimeric cytokine receptor

To express GM18 in CAR T-cells we generated a retroviral vector in which the chimeric α and β GM18 receptor chains are separated by a 2A sequence (Figure 1A,B). To initially confirm the functionality of GM18, we transduced wildtype (WT) and MyD88 knockdown (KD) NFκB/AP-1 Ramos-Blue reporter cell lines and treated GM18-transduced or unmodified reporter cells with increasing concentration of exogenous GM-CSF. Only GM18-transduced WT Ramos-Blue cells displayed NFκB activation in the presence of GM-CSF, demonstrating that GM18 is functional and that its signals through MyD88 (Figure 1C).

In order to determine if GM18 improves CAR T-cell function, we initially focused on T-cells genetically modified with a retroviral vector encoding an EphA2-CD28.ζ.CAR, a 2A sequence, and truncated CD19 (EphA2-CAR)(6). EphA2-CAR and EphA2-CAR.GM18 T-cells were generated by single or co-transduction. Anti-CD19 was used to detect T-cells transduced with the EphA2-CAR vector, and CAR expression was confirmed with an anti-F(ab_2)' showing no significant differences in regard to transduction efficiency (Supplemental Figure 1A,B). Anti-CD116 (GM-CSFRα chain) was used to identify GM18-transduced T-cells since anti-CD131 (GM-CSFRβ chain) staining consistently gave a lower % of transduction (Supplemental Figure 1C,D). Single transduction of T-cells with the EphA2-CAR vector resulted in a mean transduction efficacy of 80%, and co-transduction of T-cells with the EphA2-CAR and GM18 vectors resulted in mean of 35.4% double positive cells (Figure 1D). While the MFI of GM18 varied between donors (Supplemental Figure 1E), we sorted EphA2-CAR and EphA2-CAR.GM18 T-cells to obtain >95% pure single or double transduced cell populations based on percentage positive cells for the majority of functional

analyses unless indicated. Transduced T-cells contained a mixture of $CD4^+$ and $CD8^+$ T-cells and additional T-cell subset analysis revealed the presence of naïve, central memory, effector memory, and terminally differentiated T-cells with no significant differences when GM18 is expressed (Supplemental Figure 2A-C). To exclude that expression of GM18 induced nonspecific killing by CAR T-cells, we performed an MTS assay using the $EphA2^+$ Ewing sarcoma cell line A673 (Supplemental Figure 3) as target cells. T-cells expressing a nonfunctional EphA2-CAR (EphA2-ΔCAR) served as controls (6). While EphA2-CAR and EphA2-CAR.GM18 T-cells induced robust killing, EphA2-ΔCAR and EphA2-ΔCAR.GM18 T-cells did not (Figure 1E). To demonstrate that activating GM18 by itself does not induce T-cell expansion, we cultured non-transduced (NT) and GM18 T-cells with exogenous GM-CSF (10 or 100 ng/mL) or IL-7/IL-15. NT and GM18 T-cells only expanded in the presence of IL-7/IL-15, indicating that GM18 does not induce nonspecific T-cell expansion (Supplemental Figure 4A,B).

EphA2-CAR.GM18 T-cells have improved effector function after chronic antigen exposure *in vitro*

We next set out to compare the functionality of EphA2-CAR and EphA2-CAR.GM18 T-cells using a sequential stimulation assay to mimic chronic antigen exposure. CAR T-cells were stimulated every 7 days with A673 cells as long as they were viable and had killed all tumor cells by visual inspection. Before each stimulation, T-cells were enumerated to determine expansion, and following 48 hours after the addition of fresh tumor cells an aliquot of culture media was collected to determine the concentration of T_H1/T_C1 (GM-CSF, IFNγ, TNFα, IL-2), T_H2/T_C2 (IL-4, IL-5, IL-6, IL-10, IL-13), and IL-17 by multiplex analysis. EphA2-CAR T-cells induced tumor killing and expanded post 2-3 stimulations before their effector function deteriorated. In contrast, EphA2-CAR.GM18 T-cells killed and expanded for at least 6 stimulations (Figure 2A). After the first stimulation, EphA2-CAR and EphA2-CAR.GM18 T-cells produced high levels (>1,000 pg/mL) of GM-CSF, IFNγ, TNFα, IL-13, and IL-2 (only EphA2-CAR.GM18); intermediate levels (100-1,000 pg/mL) of IL-4, IL-5, IL-10, and IL-2 (only EphA2-CAR); and low/undetectable levels (<100 pg/mL) of IL-6, and IL-17a (Figure 2B). While EphA2-CAR.GM18 T-cells produced higher levels of cytokines, this only reached statistical significance for IL-13. Cytokine expression was dependent on expression of a functional CAR since EphA2-ΔCAR and EphA2-ΔCAR.GM18 T-cells only produced low/undetectable levels of cytokines (Figure 2B). EphA2-CAR.GM18 T-cells continued to produce robust levels of cytokines after each stimulation. T_H1/T_C1 cytokine production decreased and T_H2/T_C2 increased between the 1^{st} and 6^{th} stimulations. However, this only reached statistical significance for IL-5 and IL-13 (Figure 2C,D).

To provide further evidence that the observed benefit on expression of a functional GM18 receptor, we generated a nonfunctional GM18 receptor (ΔGM18) with no cytoplasmic signaling domains (Supplemental Figure 5A). ΔGM18 did not activate the MyD88 signaling pathway and while it did not interfere with cytokine production of EphA2-CAR T cells, it did not enhance their ability to expand in repeat stimulation assays (Supplemental Figure 5B-E). Having a ΔGM18 receptor and ΔCAR also allowed us to address the question if expression of both molecules in T-cells are required. CAR T-cells were mixed at a ratio of

1:1 with either CAR.GM18, CAR.ΔGM18, ΔCAR.GM18, or ΔCAR.ΔGM18 T-cells. This admixture of T-cells was then stimulated for 24 hours with recombinant protein, and cultured for 7 days prior to performing FACS analysis to determine the percentage of the respective CAR T-cell populations. While the percentage of CAR.GM18 and CAR.ΔGM18 T-cells remained stable, there was a significant decline for ΔCAR.GM18 and ΔCAR.ΔGM18 T cells, demonstrating that CAR activation is critical and bystander activation very unlikely (Supplemental Figure 6A,B). Finally, to explore if the benefit of GM18 could be extended to CARs with a 41BB costimulatory domain, we transduced EphA2-41BBζ.CAR T-cells (CAR^{BB} T-cells) with GM18 cells (Supplemental Figure 7A). CAR^{BB}.GM18 T-cells were functional as judged by cytokine production, and had a significant greater ability to expand than CAR^{BB} T-cells in our repeat stimulation assay (Supplemental Figure 7B-D).

EphA2-CAR.GM18 T-cells outperform EphA2-CAR T-cells *in vivo*

To assess the *in vivo* antitumor activity of EphA2-CAR.GM18 T-cells, we used the A673 Ewing sarcoma xenograft model. NSG mice were injected with $2x10^6$ A673 tumor cells subcutaneously (s.c.) and on day 7 received one single intravenous (i.v.) dose of $1x10^5$ or $3x10^5$ CAR T-cells (Figure 3A; Supplemental Figure 8). In some of the experiments, CAR T-cells were genetically modified to express GFP.ffLuc (Figure 3A). Tumor growth was monitored by caliper measurements and CAR T-cell expansion and persistence by weekly bioluminescence imaging. EphA2-CAR T-cells induced complete responses (CRs) in 4/14 (29%) mice at the lower and in 6/9 (66%) mice at the higher cell dose (Figure 3B,C; Supplemental Figure 9). In contrast, EphA2-CAR.GM18 T-cells induced CRs in 14/15 (93%) at the lower cell dose and in 10/10 mice (100%) at the higher cell dose (Figure 3B,C). Tumor recurrences after an initial CR only occurred in mice that had received $1x10^5$ EphA2-CAR T-cells (2 out 4 mice). EphA2-CAR.GM18 T-cells induced a significant survival advantage at both evaluated cell doses in comparison to untreated controls. In contrast, EphA2-CAR T-cell therapy only improved survival at the higher ($3x10^5$) cell dose (Figure 3D). CAR T-cell infused mice continued to gain weight (Supplemental Figure 10), and in long-term survivors we did not observe clinical signs of graft versus host disease (GVHD) except in 2/10 mice in the $3x10^5$ EphA2-CAR.GM18 T-cell group, requiring euthanasia at 9 weeks post T-cell injection.

Improved antitumor activity of EphA2-CAR.GM18 T-cells at a cell dose of $1x10^5$ per mouse correlated with a significant greater peak expansion in comparison to EphA2-CAR T-cells (Figure 3E,F). There was no significant difference between EphA2-CAR- and EphA2-CAR.GM18 T-cells at the higher cell dose in regard to peak T-cell expansion and persistence (Figure 3E,F). We observed increased expansion of EphA2-CAR.GM18 T-cells at the lower cell dose. Since EphA2-CAR.GM18 T-cell proliferation depends on antigen density (Supplemental Figure 11A,B), improved expansion is most likely due to the fact that the tumor to CAR T-cell ratio is higher at the lower cell dose (i.e. an individual CAR T-cell encounters more antigen). To assess the functionality of CAR T-cells in long-term survivors, we re-challenged subset of mice with A673 cells on day 100 after initial tumor cell injection (Figure 3G). Of 19 rechallenged mice post EphA2-CAR- or EphA2-CAR.GM18 T-cell therapy, only one mouse developed an EphA2-negative tumor (Figure 3H). In contrast, tumor take was 100% for naïve mice. Rejection of tumor cells did not induce expansion of

EphA2-CAR and EphA2-CAR.GM18 T-cells as judged by weekly bioluminescence imaging except in 2 mice that had received EphA2-CAR.GM18 T-cells (Supplemental Figure 12A,B).

Having established that EphA2-CAR.GM18 CAR T-cells have potent antitumor activity *in vivo*, we confirmed in additional experiment that the expression of a functional CAR and GM18 is critical for the observed benefit. A673-bearing mice received on day 7 one single intravenous (i.v.) dose of non-transduced T-cells, GM18 T-cells, ΔCAR T-cells, ΔCAR.GM18 T-cells, or CAR.GM18 T-cells, mice that received only tumor cells served as controls. Only CAR.GM18 T cells had significant antitumor activity resulting in a survival advantage (Supplemental Figure 13A-C), demonstrating that the expression of a functional CAR and GM18 is critical for the observed benefit.

GM18 improves the effector function of HER2-CAR T-cells

In the final set of experiments, we wanted to establish that the benefit of GM18 expression is not only limited to EphA2-CAR T-cells. We focused on T-cells expressing a 2nd generation HER2-CAR with a CD28.ζ signaling domain (HER2-CAR), which had been evaluated in preclinical as well as clinical studies (7-9). We generated HER2-CAR and HER2-CAR.GM18 T-cells by retroviral transduction (Figure 4A), and phenotypic analysis revealed no significant differences between CAR T-cell populations (Supplemental Figure 14A-E). The *in vitro* experiments were conducted with unsorted (N=3) and sorted T-cells (N=1), whereas the *in vivo* experiments were conducted with sorted cells. We performed our standard restimulation assay using HER2^{+} LM7 osteosarcoma cells as targets with the only exception that exogenous IL-15 (5 ng/mL) was added with each restimulation. HER2-CAR.GM18 T-cells expanded significantly more in comparison to HER2-CAR T-cells within 4 stimulations (Figure 4B,C). After the first stimulation, HER2-CAR and HER2-CAR.GM18 T-cells produced high levels (>1,000 pg/mL) of GM-CSF, IFNγ, IL-13, and TNFα (only HER2-CAR.GM18); intermediate levels (100-1,000 pg/mL) of IL-4, IL-5, and TNFα (only HER2-CAR); and low/undetectable levels (<100 pg/mL) of IL-2, IL-5, IL-6, and IL-17a (Figure 4D). HER2-CAR.GM18 T-cells produced higher levels of cytokines than HER2-CAR T-cells, but this only reached statistical significance for IL-13. HER2-CAR.GM18 T-cells, as observed for EphA2-CAR.GM18 T-cells, sustained cytokine stimulation with each stimulation (Figure 4E).

To determine if GM18 also endowed HER2-CAR T-cells with enhanced antitumor activity *in vivo*, we utilized an established osteosarcoma model where LM7.GFP.ffLuc cells were injected intraperitoneally (i.p.) into NSG mice followed by one single i.v. CAR T-cell injection on day 7 (Figure 4F). We evaluated two cell doses (1x10^{5} and 3x10^{5} T-cells) at which HER2-CAR T-cells were ineffective. In contrast, HER2-CAR.GM18 T-cells had potent antitumor activity at both cell doses resulting in a significant survival advantage (Figure 4G-I; Supplemental Figures 15-16).

DISCUSSION

Here we describe the development and characterization of an autocrine loop that links T-cell activation to the MyD88 signaling pathway, which plays a critical role in innate immunity.

To create a functional loop, we designed a chimeric cytokine receptor, GM18, that i) binds GM-CSF, a cytokine secreted upon CAR T-cell activation, and ii) signals through the IL18 receptor. CAR T-cells expressing GM18 recognized tumor cells in an antigen-dependent manner and had improved effector function *in vitro* in the setting of chronic antigen exposure in comparison to unmodified CAR T-cells. This translated into potent antitumor activity in two solid tumor xenograft model targeting EphA2 or HER2.

Several approaches are being developed to improve the antitumor activity of CAR T-cells including the expression of transcription factors, cytokines, constitutively active cytokine receptors, inducible costimulatory molecules, or chimeric cytokine or switch receptors (10-12). In addition, gene editing approaches are actively being pursued to delete negative regulators in CAR T-cells such as PD-1 (13) or Regnase-1 (14). In most studies thus far, expression of the introduced gene is not linked to T-cell activation, with the exception of studies that have utilized the nuclear factor of activated T-cells (NFAT) promoter to drive transgene expression (15-17). While effective in preclinical studies, the NFAT promoter was not sufficient to control IL-12 production by genetically-modified tumor infiltrating lymphocytes (TILs) in early phase clinical testing, resulting in systemic toxicities (16). Other regulatory systems have been developed that take advantage of small synthetic molecules or molecules that are present in the tumor microenvironment (18). Here, we decided to develop an autocrine loop to support T-cell effector function in which a constitutively expressed molecule is triggered by GM-CSF, which is consistently expressed upon CAR T-cell activation (3). Since we and other investigators had previously shown that activating MyD88 in CAR T-cells improves their effector function (3,19,20), we decided to link GM-CSF secretion to MyD88 signaling. Although MyD88 is the central signaling hub for TLRs, it is also the critical downstream signaling molecule for IL-1 and IL-18 receptors within T-cells(4). We selected the IL-18 receptor for our autocrine loop and designed a chimeric GM-CSF receptor with the transmembrane and signaling domains of IL-18R. Our design was based on a chimeric GM-CSF/IL-2 receptor, which enabled cytotoxic T-cell clones to grow *in vitro* without exogenous cytokines in an activation-dependent manner (21).

EphA2-CAR.GM18 or HER2-CAR.GM18 T-cells produced higher amounts of cytokines after the 1st exposure to tumor cells than their unmodified counterparts. However, this only reached statistical significance for IL-13. IL-13 is a T_H2/T_c2 cytokine that is implicated in dampening antitumor responses and directly promoting growth of IL13Rα2-positive tumors (22). Yet, CAR T-cells coexpressed IL-13 with T_H1 cytokines such as IFNγ and TNFα post-activation, which most likely counteracts any of its potential immunosuppressive effects or skewing toward a T_H2/T_C2 phenotype. Indeed, CAR.GM18 T-cells outperformed CAR T-cells in repeat stimulation assays as judged by their ability to expand and produce cytokines. This data suggests that the increased durability and potency of CAR.GM18 T cells may outweigh any of the potential protumorigenic effects of IL13. Nevertheless, studies in additional animal models are needed to confirm our findings. With repeat stimulations, there was no significant decrease in GM-CSF production by CAR.GM18 T-cells, indicating that our designed autocrine loop remains intact. Importantly, there was also no increase, arguing against a self-amplifying autocrine loop, which would raise safety concerns. We observed an increase in IL-5 secretion over repeat stimulations of EphA2-CAR.GM18 T-cells. Increased IL-5 has been associated with eosinophil-mediated immune modulation and metastasis in

some solid tumor models, thus warranting further investigation in immune competent models (23). Lastly, exogenous GM-CSF without T-cell activation or activated bystander CAR T cells did not induce CAR.GM18 T-cell proliferation, making it very unlikely that GM-CSF, which can be produced by endogenous cells in the tumor microenvironment (24) could induce nonspecific CAR T-cell expansion. Of interest, EphA2-CAR.GM18 T-cells required no addition of exogenous IL-15 to observe a benefit *in vitro*, whereas HER2-CAR.GM18 T-cells did. This is most likely due to differences in the strength of CAR-mediated T-cell activation since EphA2-CAR.GM18 T-cells secreted higher amounts of T_C1/T_H1 cytokines after initial tumor cell stimulation in comparison to HER2-CAR.GM18 T-cells, although this only reached statistical significance for GM-CSF (Supplemental Figure 17).

While high CAR T-cell doses ($5x10^6$ to $10x10^6$ CAR T cells per mouse) have been effective in numerous preclinical solid tumor models, clinical activity against solid has been limited. (1,2) We there focused on evaluating low doses of CAR T cells ($1x10^5$ or $3x10^5$ per mouse) to determine if transgenic expression of GM18 improves their effector function. EphA2-CAR.GM18 and HER2-CAR.GM18 T-cells outperformed EphA2- and HER2-CAR T-cells in xenograft models and induced complete remission in >90% of animals at a cell dose of $1x10^5$ T-cells per mouse at which unmodified EphA2-CAR or HER2-CAR T-cells were ineffective. In one of our models, we assessed T-cell expansion and demonstrated that improved expansion and persistence of CAR.GM18 T-cells correlated with improved antitumor activity. At an effective CAR.GM18 T-cell doses of $1x10^5$ T-cells per mouse, T-cells persisted long-term, did not induce xenogeneic GVHD, and rejected a 2^{nd} tumor challenge 3 months post-initial injection. Collectively, this indicates that modification of CAR T-cells with GM18 does not induce antigen-independent CAR T-cell expansion *in vivo*. In contrast, constitutive, transgenic expression of IL-18 in CAR T-cells improves their effector function, but also induces weight loss in some mouse models and antigen-independent T-cell function (15,25). These studies highlight that it is critical to link the MyD88 signaling pathway to T-cell activation, which we accomplished with the designed GM18 receptor. Other investigators have used the NFAT promoter to link IL-18 expression to T-cell activation (15); however, as discussed above, this promoter failed to control IL-12 production by TILs in early phase clinical testing (16). In our study we demonstrated the benefit of expressing GM18 in human CAR T cells. In the future our findings have to be confirmed in immune competent animal models especially since there is no biological cross reactivity between human and murine GM-CSF. Likewise, immune competent models will also allow us to perform additional studies focused for example on T-cell metabolism and safety.

In conclusion we designed a chimeric cytokine receptor, GM18, to establish an autocrine loop that links T-cell activation to the MyD88 signaling pathway. Expression of GM18 in CAR T-cells strikingly improved their effector function resulting in potent antitumor activity. Thus, hijacking cytokines, like GM-CSF that are secreted by T-cells in an antigen-dependent manner, for therapeutic benefit, present a viable option to improve current T-cell therapy approaches.

MATERIALS AND METHODS

Tumor cell lines

A673 (Ewing sarcoma) was purchased from the American Type Culture Collection (ATCC), and the LM7 (osteosarcoma) cell line was provided by Dr. Eugenie Kleinerman (MD Anderson Cancer Center, Houston, TX). Cell lines were authenticated by the ATCC human STR profiling cell authentication service and routinely checked for Mycoplasma by the MycoAlert Mycoplasma Detection Kit (Lonza). The generation of LM7 cells, genetically modified to express an enhanced green fluorescent protein firefly luciferase molecule (LM7.GFP.ffLuc) was previously described (7). Once thawed, cell lines were kept in culture for a maximum of three months before a new reference vial was thawed. Cell lines were maintained and expanded in DMEM (GE Healthcare Life Sciences HyClone Laboratories) supplemented with 10% fetal bovine serum (FBS; GE Healthcare Life Sciences HyClone Laboratories) and 2mM Glutamax (Invitrogen).

Generation of retroviral vectors

The generation of SFG retroviral vectors encoding EphA2-CAR-2A-tCD19, EphA2-ΔCAR-2A-tCD19, EphA2-CAR-2A-tCD19 with 41BB costimulatory domain (CAR^{BB}) or HER2-CAR have previously been described (6,7). The SFG retroviral vector encoding GM18 was generated by synthesizing gene fragments (Thermo Fisher Scientific) and In-Fusion cloning (Takara Bio). It consists of i) the GM-CSFRβ isoform 2 extracellular domain ending with amino acids MW, ii) the transmembrane domain and intracellular domain of the IL18Rβ chain starting with amino acids GV (omitting the 2^{nd} V), iii) a T2A sequence, iv) the GM-CSFRα extracellular domain ending with amino acids DG, and v) the transmembrane domain and intracellular domain of the IL-18Rα chain starting with amino acids MI. A non-signaling GM18 construct (ΔGM18) was generated by In-Fusion cloning to truncate the intracellular domains of IL18Rβ and IL18Rα to 10 amino acids (ending with amino acids IE for IL18Rβ and amino acids YR for IL18Rα). The sequences of the final constructs were verified by sequencing (Hartwell Center, St. Jude Children's Research Hospital). RD114-pseudotyped retroviral particles were generated by transient transfection of 293T-cells as previously described (6). Supernatants were collected after 48 hours, filtered, and snap frozen.

Generation of CAR and CAR.GM18 T-cells

Human peripheral blood mononuclear cells (PBMCs) were obtained from whole blood of healthy donors under an IRB approved protocol at St. Jude Children's Research Hospital, after written informed consent was obtained in accordance with the Declaration of Helsinki or from de-identified donor pheresis products of St. Jude Blood Donor Center. Retroviral transduced T-cells were generated as previously described (6). Briefly, PBMCs were stimulated on anti-CD3 and anti-CD28 coated plates for 48 hours. Recombinant human IL-7 (10 ng/mL, Peprotech) and IL-15 (5 ng/mL, Peprotech) were added 24 hours after initial stimulation and were maintained in culture until functional studies were performed. Cells were then seeded onto retronectin-coated (Clontech) plates with retroviral particles for 2-4 days for transduction. Non-transduced T-cells (NT) were prepared similarly except no retrovirus was included in the retronectin wells. To generate CAR.GM18 and CAR.ΔGM18

T-cells, T-cells were co-transduced with both retroviral particles in the same well. For generation of EphA2-CAR-GFP.ffLuc and EphA2-CAR.GM18-GFP.ffLuc T-cells, activated T-cells were first transduced with CAR or CAR+GM18 for 24 hours, and then transferred to GFP.ffLuc retrovirus-containing retronectin-coated plate for 3-4 days. T-cells were then expanded and sorted for functional analysis for 7-10 days post-transduction. For all *in vitro* and *in vivo* experiments in which the effector function of CAR and CAR.GM18 T-cells was compared, T cells from the same donor were transduced with i) CAR-encoding retroviral particles or ii) a mixture of CAR- and GM18-encoding retroviral particles. All T-cells were cultured with RPMI-1640 supplemented with 10% FBS and 2mM Glutamax (complete RPMI).

Flow cytometry and cell sorting

Surface staining: The FACSCanto II instrument (BD Biosciences) was used for acquisition and FlowJo v10 (FlowJo) was used for analysis of flow cytometry data. Samples were washed with and stained in PBS (Lonza) with 1% FBS. For all experiments, known negatives (e.g. NT T-cells) served as gating controls. eBioscience Fixable viability dyes (Invitrogen) were used to exclude dead cells from analysis. T-cells were evaluated for CAR expression 5-10 days post transduction using anti-CD19 (J3-119, Beckman Coulter; SJ25C1, BD Biosciences) or anti-human IgG $F(ab')_2$ fragment specific antibody (Jackson ImmunoResearch) for EphA2-CAR. Anti-mouse IgG $F(ab')_2$ fragment specific antibody (Jackson ImmunoResearch) was used to detect HER2-CAR expression. GM18 expression was analyzed by staining with anti-CD116 (4H1, BioLegend). CAR T-cell phenotype was established using the following antibodies: CD4 (SK3, BD Biosciences), CD8 (HIT8a, BD Biosciences), CD45RA (HI100, BD Biosciences), and CCR7 (G043H7, BioLegend; 150503, BD Biosciences). The beta chain of GM18 was detected with anti-CD131 (3D7, BD Biosciences). Cell surface EphA2 expression was detected using anti-EphA2 (371805, R&D Systems).

Sorting: For functional studies, cells were sorted on a BD FACS Aria III cell sorter (BD Biosciences). Cells were stained for anti-CD19-APC (J3-119, Beckman Coulter; EphA2-CAR) or anti-mouse IgG $F(ab')_2$ fragment specific-AlexaFluor 647 (HER2-CAR) plus anti-CD116-PE (4H1, BioLegend or hGM-CSFR-M1, BD Biosciences). DAPI (Thermo Fisher) was used as a viability indicator. Cells were rested 48-72 hours in RPMI containing 20% FBS, 25 μg/ml gentamicin (Gibco), 1X penicillin-streptomycin (Gibco), and 1.5 μg/ml amphotericin B (Gibco) prior to functional assays.

Ramos-Blue™ NFκB reporter assay

Ramos-Blue™ (WT) and Ramos-Blue™ KD-MyD (MyD88 knockdown, KD) NF-κB/AP-1 reporter B lymphocytes (InvivoGen) were transduced with GM18, ΔGM18 or not transduced (NT) and expanded per manufacturer instructions. $4x10^5$ NT or GM18 Ramos-Blue™ cells were seeded in a 96-well plate in IMDM (Gibco) with 10% FBS (GE Healthcare Life Sciences HyClone Laboratories) and stimulated with exogenous recombinant human GM-CSF (R&D Systems) at titrated concentrations for 24 hours. Supernatant was collected and incubated with QUANTI-BLUE™ solution (InvivoGen) for 2 hours. Colorimetric changes

were then detected via absorbance at 640 nm using an Infinite® 200 Pro MPlex plate reader (Tecan).

Repeat stimulation assay

$1x10^6$ (or $5x10^5$) T-cells were cocultured in complete RPMI with $5x10^5$ (or $1x10^5$) tumor cells in a 24-well or 48-well tissue culture-treated plate, respectively. IL-15 (5 ng/ml) was added to HER2-CAR T-cell experiments. Cells were fed with fresh complete RPMI at 48 and 120 hours after coculture. After 7 days, T-cells were harvested, counted, and replated at the same ratio with fresh tumor cells as long as they had killed tumor cells by microscopic inspection.

Analysis of cytokine production

Supernatants from repeat stimulation assays were collected 48 hours after each new stimulation and frozen at −80°C. Cytokines and chemokines were then quantified using a MILLIPLEX MAP Human Cytokine/Chemokine Magnetic Bead Panel kit (EMD Millipore) on a FLEXMAP 3D System (Luminex).

Exogenous GM-CSF treatment of T-cells

Eight days post-transduction, NT or GM18 T-cells were plated with recombinant human IL-7 (10 ng/mL, Peprotech) and IL-15 (5 ng/mL, Peprotech), recombinant human GM-CSF (100 ng/mL or 10 ng/mL, R&D Systems), or no exogenous cytokines for 5 days. Cells were then enumerated and the frequency of $GM18^+$ cells were determined by flow cytometry.

MTS assay

A CellTiter96® AQueous One Solution Cell Proliferation Assay (Promega) was utilized to assess CAR T-cell cytotoxicity. In a tissue culture-treated 96-well plate, 19,000 A673 cells were co-cultured with serial dilutions of CAR T-cells. Media only and tumor cells alone served as controls. Each condition was plated in technical triplicates. After 24 hours, the media and T-cells were removed by gently pipetting up and down to avoid disrupting adherent tumor cells. CellTiter96® AQueous One Solution Reagent (phenazine ethosulfate) in complete RPMI was added to each well and incubated at 37°C for 3 hours. The absorbance at 492 nm was measured using an Infinite® 200 Pro MPlex plate reader (Tecan) to quantify the viable cells in each well. Percent live tumor cells were determined by the following formula: (sample-media only)/(tumor alone-media only)*100.

Xenograft mouse models

All animal experiments were approved by St. Jude Children's Research Hospital Institutional Animal Care and Use Committee (IACUC). Xenograft experiments were performed with 7-10 week old NOD-*scid* IL2Rgamma^{null} (NSG) mice obtained from St. Jude Children's Research Hospital NSG colony. A673 Ewing sarcoma model: Mice received s.c. injection of $2x10^6$ A673 cells in Matrigel (Corning) in the right flank. On day 7, mice received a single i.v. dose of $1x10^5$ or $3x10^5$ EphA2-CAR or EphA2-CAR.GM18 T-cells via tail vein injection. Tumor growth was measured by weekly caliper measurements. Mice were euthanized when they met physical euthanasia criteria (significant weight loss, signs of

distress), when the tumor burden reached 20% of total body mass (≥4000 mm^3), or when recommended by veterinary staff. For rechallenge experiments, mice received an additional s.c. injection of $2x10^6$ A673 cells in the left flank between days 102 to 104 after initial tumor cell injection. LM7 osteosarcoma model: Mice were injected i.p. with $1x10^6$ LM7.GFP.ffLuc cells, and on day 7 received a single i.v. dose of $1x10^5$ or $3x10^5$ HER2-CAR or HER2-CAR.GM18 T-cells via tail vein injection. Mice were euthanized when they reached our bioluminescence flux endpoint of $1x10^{10}$ for 2 consecutive weeks, and/or the above-mentioned general euthanasia criteria.

Bioluminescence imaging

Mice were injected i.p. with 150 mg/kg of D-luciferin 5-10 minutes before imaging, anesthetized with isoflurane, and imaged with a Xenogen IVIS-200 imaging system. The photons emitted from the luciferase-expressing tumor cells were quantified using Living Image software (Caliper Life Sciences). Mice were imaged once per week to track either T-cells (EphA2-CAR T-cell experiments) or LM7 tumor burden (HER2-CAR T-cell experiments).

Statistical analysis

For all experiments, the number of biological replicates and statistical analysis used are described in the figure legend. For comparison between two groups, a two-tailed t-test was used. For comparisons of three or more groups, values were log transformed as needed and analyzed by ANOVA with Dunnett's or Tukey's post-test. Survival was assessed by the log-rank test with Bonferroni adjustment for multiple comparisons. Bioluminescence imaging data were analyzed using either ANOVA or area under the curve (AUC). Statistical analyses were conducted with Prism software (GraphPad Software, San Diego, CA).

Supplementary Material

Refer to Web version on PubMed Central for supplementary material.

ACKNOWLEDGMENTS

The authors would like to thank Krista Millican and Amanda George (St. Jude Animal Resource Center) and Rebecca Thorne (St. Jude Center for In Vivo Imaging and Therapeutics) for assistance with in vivo mouse studies. The schematic (Figure 1B) was created with BioRender (Biorender.com) for which we have license.

Funding: The work was supported by the Alex Lemonade Stand Foundation and the American Lebanese Syrian Associated Charites. Animal imaging was performed by the Center for In Vivo Imaging and Therapeutics, which is supported in part by National Institutes of Health (NIH) grants P01CA096832 and R50CA211481. Cellular images were acquired at SJCRH Cell & Tissue Imaging Center which is supported by St. Jude and National Cancer Institute (NCI) P30 CA021765. The content is solely the responsibility of the authors and does not necessarily represent the official views of the NIH.

REFERENCES

1. Majzner RG, Mackall CL. Clinical lessons learned from the first leg of the CAR T cell journey. Nat Med 2019;25(9):1341–55 doi 10.1038/s41591-019-0564-6. [PubMed: 31501612]
2. Rafiq S, Hackett CS, Brentjens RJ. Engineering strategies to overcome the current roadblocks in CAR T cell therapy. Nat Rev Clin Oncol 2020;17(3):147–67 doi 10.1038/s41571-019-0297-y. [PubMed: 31848460]

3. Mata M, Gerken C, Nguyen P, Krenciute G, Spencer DM, Gottschalk S. Inducible Activation of MyD88 and CD40 in CAR T Cells Results in Controllable and Potent Antitumor Activity in Preclinical Solid Tumor Models. Cancer Discov 2017;7(11):1306–19 doi 10.1158/2159-8290.CD-17-0263. [PubMed: 28801306]

4. Deguine J, Barton GM. MyD88: a central player in innate immune signaling. F1000Prime Rep 2014;6:97 doi 10.12703/P6-97. [PubMed: 25580251]

5. Roybal KT, Williams JZ, Morsut L, Rupp LJ, Kolinko I, Choe JH, et al. Engineering T Cells with Customized Therapeutic Response Programs Using Synthetic Notch Receptors. Cell 2016;167(2):419–32 e16 doi 10.1016/j.cell.2016.09.011. [PubMed: 27693353]

6. Yi Z, Prinzing BL, Cao F, Gottschalk S, Krenciute G. Optimizing EphA2-CAR T Cells for the Adoptive Immunotherapy of Glioma. Mol Ther Methods Clin Dev 2018;9:70–80 doi 10.1016/j.omtm.2018.01.009. [PubMed: 29552579]

7. Ahmed N, Salsman VS, Yvon E, Louis CU, Perlaky L, Wels WS, et al. Immunotherapy for osteosarcoma: genetic modification of T cells overcomes low levels of tumor antigen expression. Mol Ther 2009;17(10):1779–87 doi 10.1038/mt.2009.133. [PubMed: 19532139]

8. Ahmed N, Brawley VS, Hegde M, Robertson C, Ghazi A, Gerken C, et al. Human Epidermal Growth Factor Receptor 2 (HER2) -Specific Chimeric Antigen Receptor-Modified T Cells for the Immunotherapy of HER2-Positive Sarcoma. J Clin Oncol 2015;33(15):1688–96 doi 10.1200/JCO.2014.58.0225. [PubMed: 25800760]

9. Ahmed N, Brawley V, Hegde M, Bielamowicz K, Kalra M, Landi D, et al. HER2-Specific Chimeric Antigen Receptor-Modified Virus-Specific T Cells for Progressive Glioblastoma: A Phase 1 Dose-Escalation Trial. JAMA Oncol 2017;3(8):1094–101 doi 10.1001/jamaoncol.2017.0184. [PubMed: 28426845]

10. DeRenzo C, Gottschalk S. Genetic Modification Strategies to Enhance CAR T Cell Persistence for Patients With Solid Tumors. Front Immunol 2019;10:218 doi 10.3389/fimmu.2019.00218. [PubMed: 30828333]

11. Lynn RC, Weber EW, Sotillo E, Gennert D, Xu P, Good Z, et al. c-Jun overexpression in CAR T cells induces exhaustion resistance. Nature 2019;576(7786):293–300 doi 10.1038/s41586-019-1805-z. [PubMed: 31802004]

12. Tian Y, Li Y, Shao Y, Zhang Y. Gene modification strategies for next-generation CAR T cells against solid cancers. J Hematol Oncol 2020;13(1):54 doi 10.1186/s13045-020-00890-6. [PubMed: 32423475]

13. Rupp LJ, Schumann K, Roybal KT, Gate RE, Ye CJ, Lim WA, et al. CRISPR/Cas9-mediated PD-1 disruption enhances anti-tumor efficacy of human chimeric antigen receptor T cells. Sci Rep 2017;7(1):737 doi 10.1038/s41598-017-00462-8. [PubMed: 28389661]

14. Wei J, Long L, Zheng W, Dhungana Y, Lim SA, Guy C, et al. Targeting REGNASE-1 programs long-lived effector T cells for cancer therapy. Nature 2019;576(7787):471–6 doi 10.1038/s41586-019-1821-z. [PubMed: 31827283]

15. Chmielewski M, Abken H. CAR T Cells Releasing IL-18 Convert to T-Bet(high) FoxO1(low) Effectors that Exhibit Augmented Activity against Advanced Solid Tumors. Cell Rep 2017;21(11):3205–19 doi 10.1016/j.celrep.2017.11.063. [PubMed: 29241547]

16. Zhang L, Morgan RA, Beane JD, Zheng Z, Dudley ME, Kassim SH, et al. Tumor-infiltrating lymphocytes genetically engineered with an inducible gene encoding interleukin-12 for the immunotherapy of metastatic melanoma. Clin Cancer Res 2015;21(10):2278–88 doi 10.1158/1078-0432.CCR-14-2085. [PubMed: 25695689]

17. Zhang L, Kerkar SP, Yu Z, Zheng Z, Yang S, Restifo NP, et al. Improving adoptive T cell therapy by targeting and controlling IL-12 expression to the tumor environment. Mol Ther 2011;19(4):751–9 doi 10.1038/mt.2010.313. [PubMed: 21285960]

18. Brandt LJB, Barnkob MB, Michaels YS, Heiselberg J, Barington T. Emerging Approaches for Regulation and Control of CAR T Cells: A Mini Review. Front Immunol 2020;11:326 doi 10.3389/fimmu.2020.00326. [PubMed: 32194561]

19. Foster AE, Mahendravada A, Shinners NP, Chang WC, Crisostomo J, Lu A, et al. Regulated Expansion and Survival of Chimeric Antigen Receptor-Modified T Cells Using Small Molecule-

Dependent Inducible MyD88/CD40. Mol Ther 2017;25(9):2176–88 doi 10.1016/j.ymthe.2017.06.014. [PubMed: 28697888]

20. Prinzing B, Schreiner P, Bell M, Fan Y, Krenciute G, Gottschalk S. MyD88/CD40 signaling retains CAR T cells in a less differentiated state. JCI Insight 2020;5(21) doi 10.1172/jci.insight.136093.
21. Evans LS, Witte PR, Feldhaus AL, Nelson BH, Riddell SR, Greenberg PD, et al. Expression of chimeric granulocyte-macrophage colony-stimulating factor/interleukin 2 receptors in human cytotoxic T lymphocyte clones results in granulocyte-macrophage colony-stimulating factor-dependent growth. Hum Gene Ther 1999;10(12):1941–51 doi 10.1089/10430349950017301. [PubMed: 10466628]
22. Terabe M, Park JM, Berzofsky JA. Role of IL-13 in regulation of anti-tumor immunity and tumor growth. Cancer Immunol Immunother 2004;53(2):79–85 doi 10.1007/s00262-003-0445-0. [PubMed: 14610620]
23. Zaynagetdinov R, Sherrill TP, Gleaves LA, McLoed AG, Saxon JA, Habermann AC, et al. Interleukin-5 facilitates lung metastasis by modulating the immune microenvironment. Cancer Res 2015;75(8):1624–34 doi 10.1158/0008-5472.CAN-14-2379. [PubMed: 25691457]
24. Dolcetti L, Peranzoni E, Ugel S, Marigo I, Fernandez Gomez A, Mesa C, et al. Hierarchy of immunosuppressive strength among myeloid-derived suppressor cell subsets is determined by GM-CSF. Eur J Immunol 2010;40(1):22–35 doi 10.1002/eji.200939903. [PubMed: 19941314]
25. Hu B, Ren J, Luo Y, Keith B, Young RM, Scholler J, et al. Augmentation of Antitumor Immunity by Human and Mouse CAR T Cells Secreting IL-18. Cell Rep 2017;20(13):3025–33 doi 10.1016/j.celrep.2017.09.002. [PubMed: 28954221]

STATEMENT OF SIGNFICANCE

We designed a chimeric cytokine receptor (GM18) that links CAR T-cell activation to MyD88 signaling. GM18 endows CAR T-cells with sustained effector function in the setting of chronic antigen exposure, resulting in potent antitumor activity in preclinical solid tumor models.

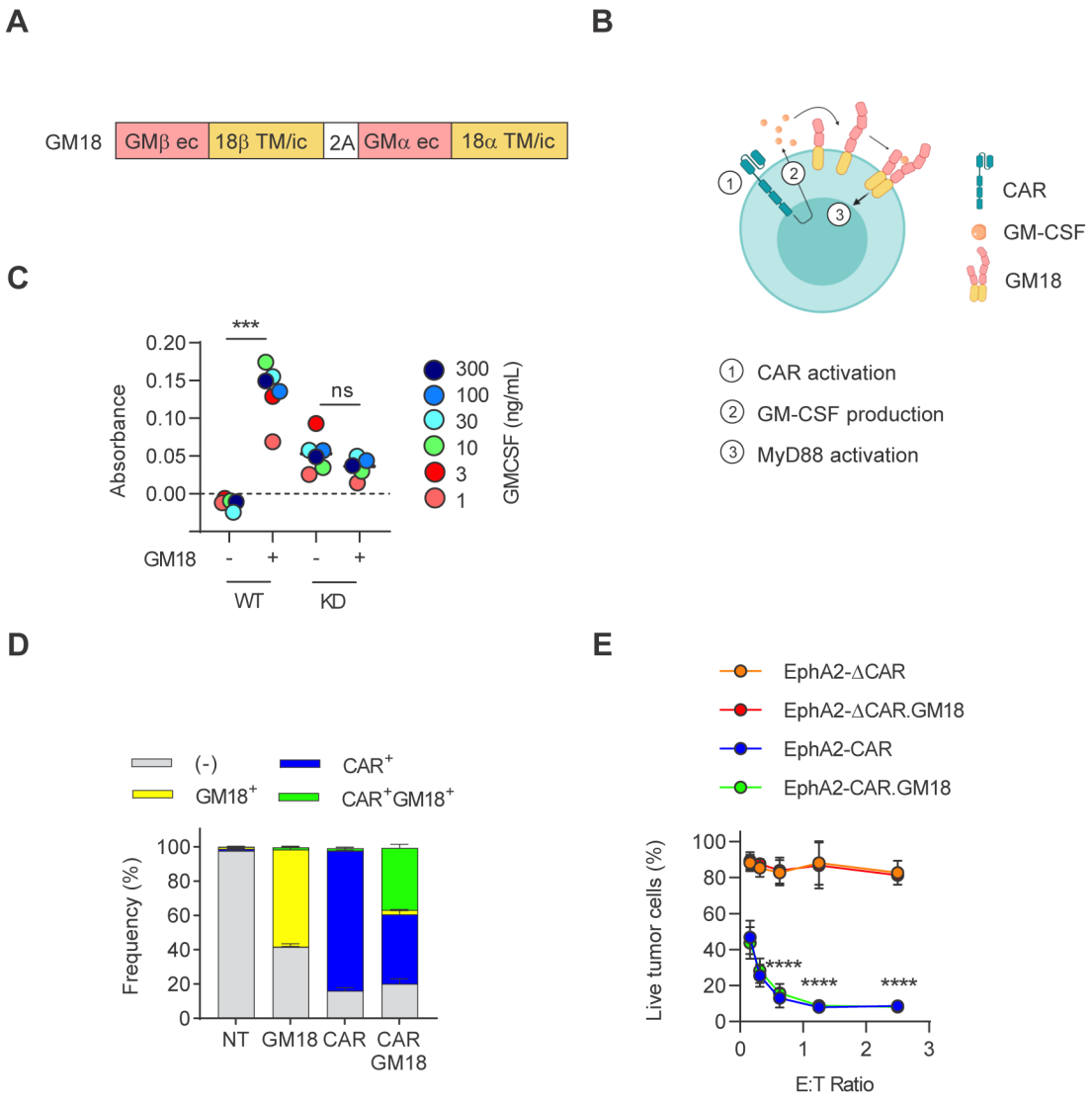

Figure 1: Generation of CAR T-cells expressing a GM-CSF:IL-18 chimeric cytokine receptor.

(**A**) Schematic of GM18 construct; GM: GM-CSF receptor; 18: IL-18 receptor; ec: extracellular domain, TM: transmembrane, ic: intracellular domain. (**B**) Schematic of GM18 signaling in CAR T-cells. CAR activation induces production of GM-CSF, and binding of GM-CSF to GM18 induces MyD88 signaling. (**C**) Colorimetric detection of NFκB activity in GM-CSF-treated wild-type (WT) or MyD88 knocked down (KD) Ramos-Blue reporter cells; ***p=0.0002; paired t-test. (**D**) Transduction efficiency of EphA2-CAR and GM18 in human T-cells (N=11) as measured by flow analysis for the GM-CSFR alpha chain (anti-CD116) and CAR (anti-CD19). NT: non-transduced. (**E**) MTS assay after 24 hour coculture of A673 tumor cells with CAR or CAR.GM18 T-cells. EphA2-ΔCAR construct was used as a non-functional control. N=3; ****p<0.0001; two-way ANOVA. For all panels, N indicate different donors.

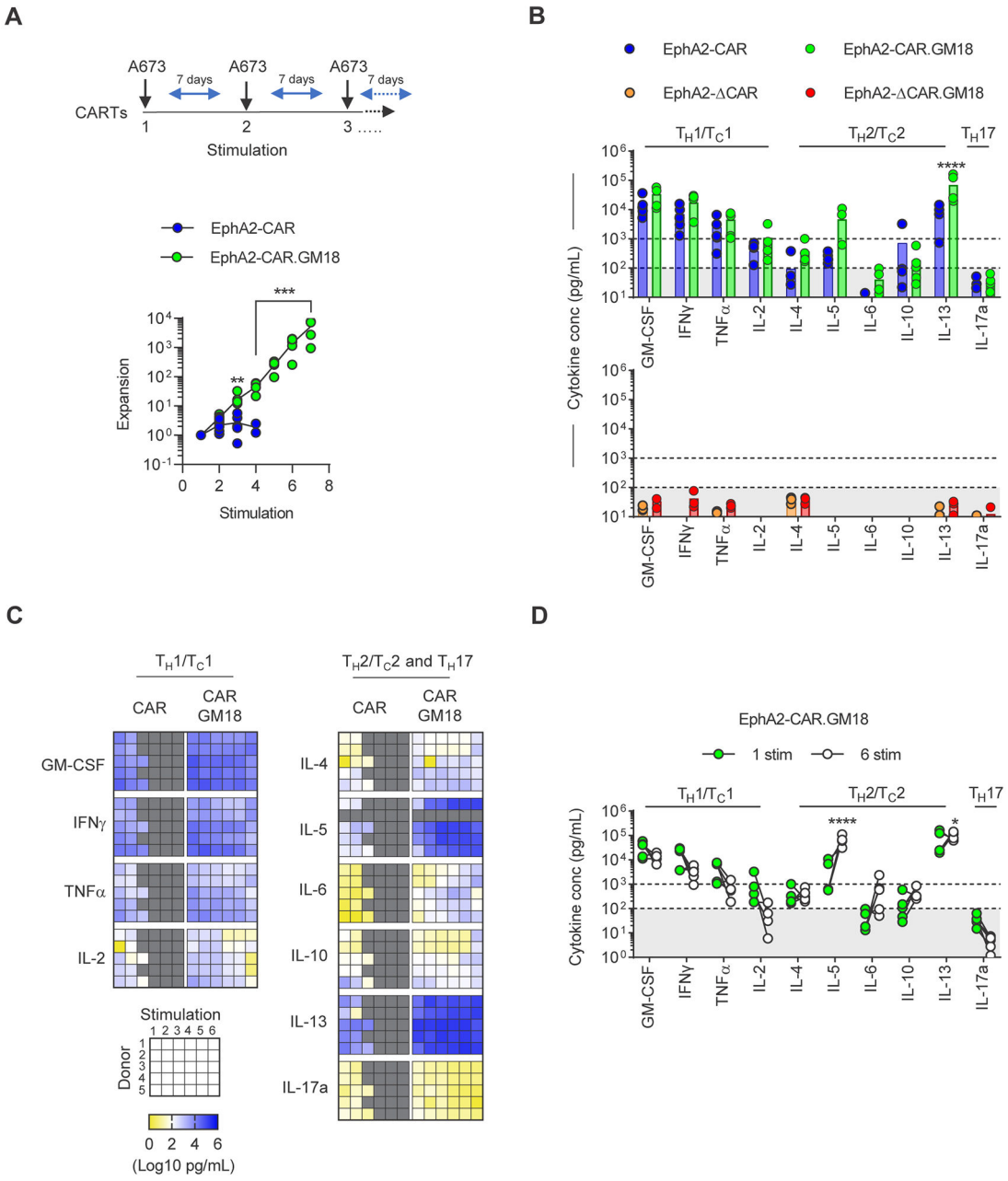

Figure 2: EphA2-CAR.GM18 T-cells have improved effector function after chronic antigen exposure i*n vitro*.

(**A**) CAR T-cell expansion following serial coculture with fresh A673 tumor cells weekly. Fold expansion of EphA2-CAR and EphA2-CAR.GM18 T-cells; N=6, **p=0.0023, **p=0.0001, paired t-test. (**B**) Cytokine production by CAR T-cells after one stimulation with A673 tumor cells at 2:1 E:T ratio measured by multiplex analysis: EphA2-CAR (N=5), EphA2-CAR.GM18 (N=5), EphA2-ΔCAR (N=3), and EphA2-ΔCAR.GM18 (N=3). (**C**) Multiplex analysis of cytokine production of CAR T-cells after 48 hours of weekly restimulation with A673 cells at 2:1 E:T ratio. IL-5: N=4, all other cytokines N=5; sorted CAR and CAR.GM18 T-cells (N=4); unsorted CAR and CAR.GM18 T-cells (N=1); double

gradient heatmap (yellow: 10^0 pg/mL, white: 10^2 pg/mL, blue 10^6 pg/mL). (**D**) Comparison of cytokine secretion between the first and sixth stimulation of EphA2-CAR.GM18 T-cells from panel C. *p=0.023, ****p<0.0001; two-way ANOVA. For all panels, N indicate different donors.

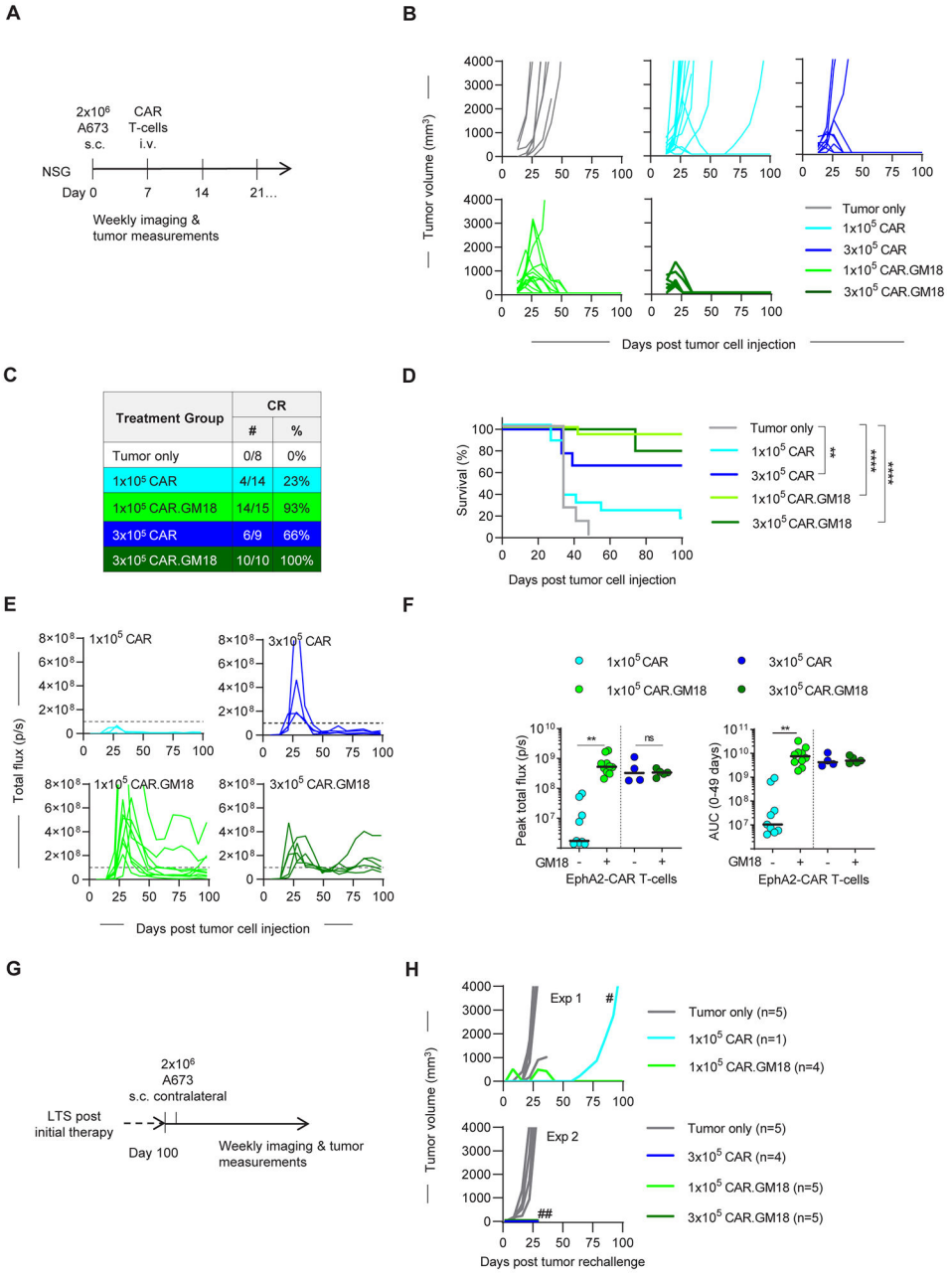

Figure 3: EphA2-CAR.GM18 T-cells outperform EphA2-CAR T-cells *in vivo*.

(**A**) NSG mice were injected with $2x10^6$ A673 cells s.c. followed by i.v. injection of CAR T-cells on day 7. Mice were imaged weekly and tumors were measured by calipers. (**B**) Tumor volume of untreated (N=8), $1x10^5$ EphA2-CAR (N=14 mice, 3 different donors), $3x10^5$ EphA2-CAR (N=9, 2 different donors), $1x10^5$ EphA2-CAR.GM18 (N=15, 3 different donors), and $1x10^5$ EphA2-CAR.GM18 (N=10, 2 different donors) T-cell treated mice. (**C**) Complete responses (CRs) in CAR treatment groups. (**D**) Kaplan-Meier survival curve; **p=0.0043, ****p<0.0001, Log-rank (Mantel-Cox) test. (**E**) Bioluminescence analysis of total flux in CAR.ffLuc T-cell treated mice. Dashed line indicates $1x10^8$; EphA2-CAR: $1x10^5$ (N=9, 2 different donors); $3x10^5$ (N=4, 1 donor); EphA2-CAR.GM18: $1x10^5$ (N=10,

2 different donors); $3x10^5$ (N=5, 1 donor). (**F**) Left panel: Peak T-cell expansion as judged by peak flux values; **p<0.0016; unpaired t-test; right panel: area under the curve (AUC) analysis until day 49 post tumor cell injection; **p<0.0059; ns: not significant, unpaired t-test. (**G**) Long term survivors (LTS) were rechallenged with a single dose of $2x10^6$ A673 cells on the contralateral side between days 102 to 104 post initial tumor cell injection. (**H**) Two independent experiments with LTS mice are shown; #: tumor was EphA2 negative; ##: experiment was terminated on day 23 post tumor rechallenge due to COVID19.

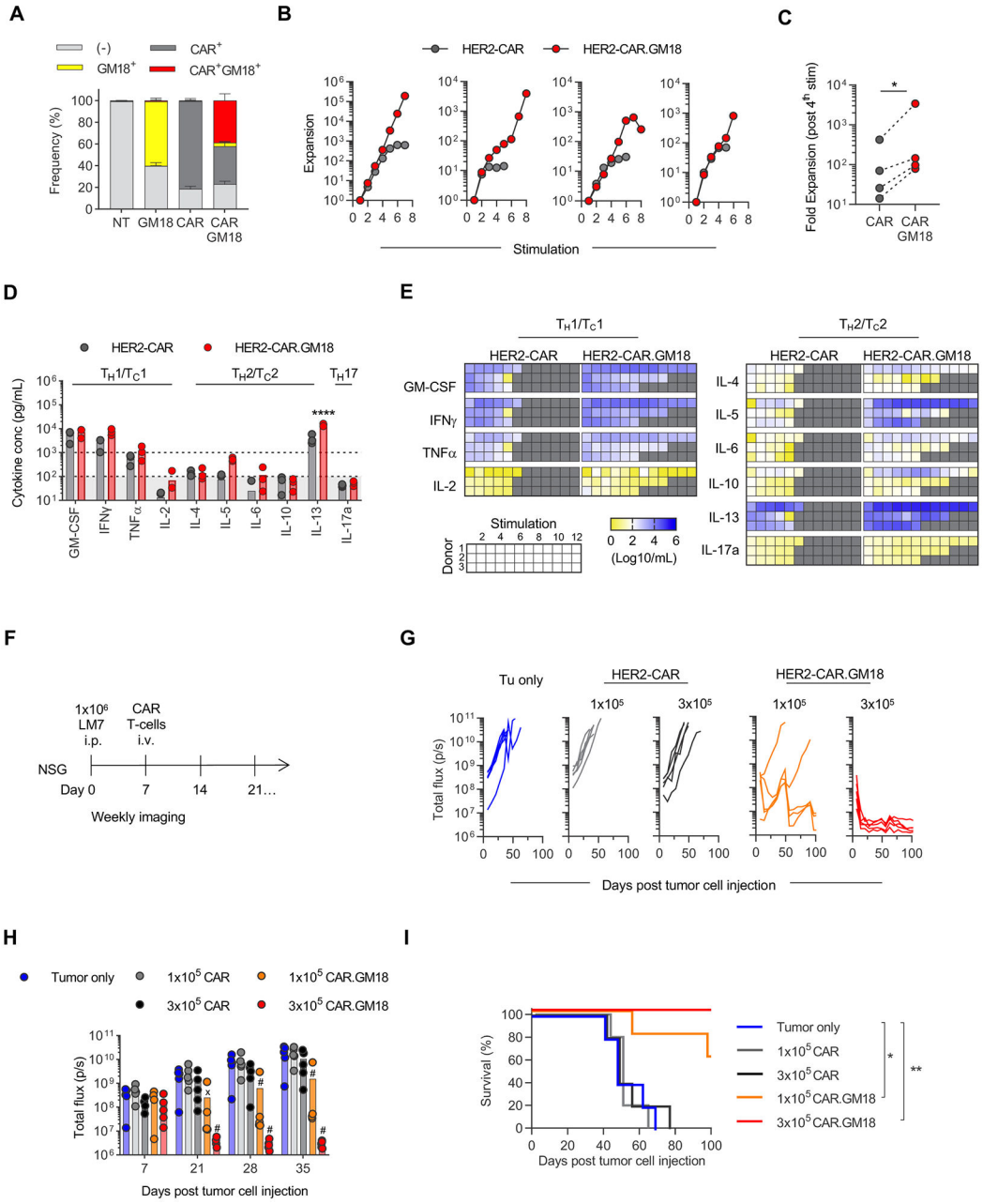

Figure 4: GM18 improves the effector function of HER2-CAR T-cells.

(**A**) Transduction efficiency of HER2-CAR and GM18 in human T-cells as measured by flow analysis for the GM-CSFR alpha chain (anti-CD116) and CAR (anti-murine F(ab')$_2$). NT: non-transduced. NT and GM18 T-cells (N=3 different donors); CAR and CAR.GM18 T-cells (N=6 different donors). (**B**) Fold expansion of HER2-CAR and HER2-CAR.GM18 T-cells following serial coculture with LM7 tumor cells weekly and IL-15 (N=4 different donors; panels 1-3 unsorted T-cells, panel 4 sorted T-cells). (**C**) Expansion from 1st to 4th simulation; p=0.0149; paired t-test. (**D**) Quantification of cytokine production by CAR T-cells after one stimulation with LM7 tumor cells. (**E**) Cytokine production by HER2-CAR and HER2-CAR.GM18 T-cells after repeat stimulations; double gradient heatmap (yellow:

10^0 pg/mL, white: 10^2 pg/mL, blue 10^6 pg/mL). (**F**) NSG mice were injected with $1x10^6$ LM7-ffLuc i.p. followed by i.v CAR T-cells on day 7 (N=5 per group, 1 donor). (**G**) Bioluminescence analysis of total flux in LM7-ffLuc tumor-bearing mice. (**H**) Comparison of tumor burden as measured by total flux at different time points. Tumor only vs $1x10^5$ or $3x10^5$ HER2-CAR.GM18 T-cells; $^{X}p=0.0017$, $^{\#}p<0.0001$; two-way ANOVA. (**I**) Kaplan-Meier survival curve; *p=0.0132, **p=0.0018, Log-rank (Mantel-Cox) test.